

On Graph Representation and Ground Surface Profiles while a Shrimp-Designed Robot is Traveling on Unexpected Landscapes

Ahmad Y. B. Hashim

Department of Robotics and Automation, Faculty of Manufacturing Engineering, Universiti Teknikal Malaysia Melaka, 76100 Durian Tnggal, Melaka, Malaysia
Email: yusairi@utem.edu.my

Abstract—Mobile robots with shrimp design are known to be dynamic when climbing or working under rugged terrains. Due to its sturdiness, robots with shrimp configuration will be able to perform difficult tasks. This work reproduced and modified a mobile robot with shrimp structural design. A typical shrimp robot has six wheels. Its structural complexity results in a perception that it is a hard-to-build robot. For straightforwardness, our shrimp rover is represented by a graph. It has a platform module attached to two forks, at front and rear, respectively. The forks have additional suspensions, whereas the platform depends on the suspension provided by the wheels. It is known that gyroscopic effects on the rover are due to ground surface conditions. The gyroscopic effects may be analyzed by computing the joint angles and change in heights during a rover maneuver. The products of joint angle and change in height represent membership functions, which values are within certain limits. A set of decision rules were developed that define an instantaneous behavior of the robot while traveling.

Index Terms—mobile robot, ground surface profile, shrimp configuration

I. INTRODUCTION

Mobile robots with shrimp design are known to be ever changing when climbing or working under rough terrains. Because of its sturdiness, robots with shrimp configuration will be able to perform complicated tasks that involucre rough terrains. Tunnel power cables, for example, has a rigor background condition. A conventional mobile robot could not be able to maneuver successfully under this situation. Sonyi *et al.* [1] used a shrimp rover to monitor tunnel power cables where it gathers real-time information about the aging status of tunnel power cables throughout operation.

The shrimp robot design is inspired from existing rover concepts. Anyhow, its main difference is the generalized use of parallel suspension architectures principal to a highly smooth slope of the center of gravity even when overcoming impediments with vertical slopes. The robot is therefore, able to move in highly rough terrain with

minimal motor power even though the friction coefficient of the ground is pretty low [2].

Although a shrimp robot might be effective under unstructured background, the control approaches should complete the overall robot's efficiency. This is usually materialized using loads of types of revolutionary algorithms where they generate the fittest data solution to the controllers. The mechanical inefficiencies might be ignored since the algorithms will compensate the errors. Such algorithm may be found throughout the work of Hassanzadeh *et al.* [3] where they applied the shuffled frog leaping optimization (SFL) algorithm to enable a mobile robot to navigate by ways of static impediments and discovered its path to reach from its initial position in the target without collision.

However, the requirement for exact formulation of system dynamics incorporating every single moving part of the robot is vital, mainly for quicker movement and concise applications. Going after this premise, Nandy *et al.* [4] proposed ever-changing formulation based on overall robot's kinetic energy in conjunction with an advanced control scheme. They claimed that actuator dynamics were considered to accomplish precise motion control, principal to a basic controller with a low-cost sensor suite. In doing so, a modular approach was adopted to derive the kinetic energy of the robot accurately and thereafter to evaluate needed equations of motion. Lamon *et al.* [5] argued that navigating in rough terrain is a complex activity. It needs the robot to be considered as a holistic system. Algorithms, on the other hand, do not consider the physical dimensions and abilities of the robot. This can conduct to inefficient motion and undergo from a lack of robustness. They suggested that a physical model of the robot is needed for trajectory control.

On the other hand, recent developments reach to the points where robots shall have their own genome in which a special personality is encoded. It is easily known as genetic robotics that combines the computational and physical systems. Genetic robot has its own genetic codes to represent a special personality, which then realize cognitive intelligence, social intelligence, behavioral intelligence, ambient intelligence, genetic intelligence and swarm intelligence [6]. The aspiration of this paper is to present a partial accomplishment from an analysis

project that studies shrimp robot design, construction, and implementation on rugged terrains. This partial accomplishment will clarify the steps to create a shrimp rover, except its control system. This work reproduced a shrimp robot based upon the design proposed by Siegwart *et al.* [2].

II. BACKGROUND

Fig. 1 exhibits that robot's model showing the forces (N) acting in a normal direction to the wheels while maneuvering, proposed by Siegwart *et al.* [2]. The

simplified model, in Fig. 1, shows the representation of the static interaction of the robot with respect to the ground. There are three subsystems, the front fork signified by a spring suspended arm rotating around O_1 , and the robot's main chassis with the real wheel. The total mass of the robot is modeled by the central body mass O_2 , and the robots main chassis with the real wheel. The total mass of the robot is modeled by the central body mass (M) and the four masses (m) of the one at a time motorized wheels.

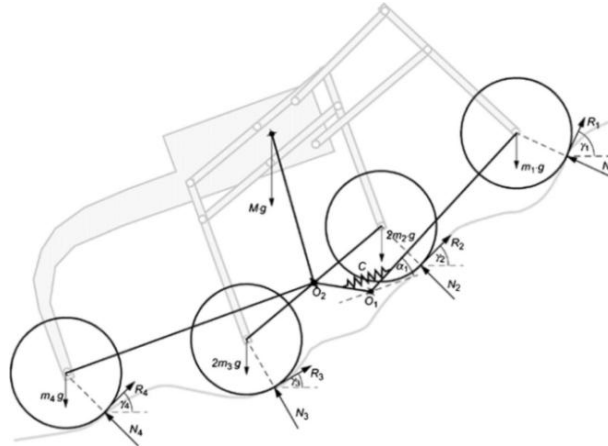


Figure 1. A simplified model of shrimp robot showing the ground reaction forces acting on the wheels. These forces resulted in the joints' responses where the robot will configure to accommodate in line with the ground contour (figure source: [2]).

The two bogies are moving symmetrically and is simplified to one bogie placed in the same plane as the front and rear wheel. The parallel structure of the front fork is modeled by a spring-suspended arm, which is rotating around the center of rotation O_1 . Assuming that there is an equal friction coefficient (μ) for each wheel, we have friction force $R = \mu N$. Therefore, (1) defines the robot's static force equilibrium.

In reference to (1), the robot responds to the degrees of ground reaction forces (f) during which the joints revolve accordingly and is proportional to the angles of attack (γ). The robot will initiate to topple if the joint rotations exceed the joints' limit. While the design is meant to counter unstructured background, it has limits to a maneuvering operation. The notation τ_1 represents the internal torque around O_1 due to the front fork suspension.

$$\left. \begin{aligned} N_1(\Delta_{N1}^{O1} + \mu\Delta_{R1}^{O1}) &= \tau_1 + mg\Delta_{m1}^{O1} \dots\dots\dots(a) \\ N_2(\mu\Delta_{R2}^{O2} + \Delta_{N2}^{O2}) + N_3(\mu\Delta_{R3}^{O2} - \Delta_{N3}^{O2}) &= 0 \dots\dots\dots(b) \\ N_1(\mu \cos \gamma_1 - \sin \gamma_1) + N_2(\mu \cos \gamma_2 - \sin \gamma_2) + \\ N_3(\mu \cos \gamma_3 - \sin \gamma_3) + N_4(\mu \cos \gamma_4 - \sin \gamma_4) &= 0 \dots(c) \\ N_1(\mu \sin \gamma_1 + \cos \gamma_1) + N_2(\mu \sin \gamma_2 + \cos \gamma_2) + \\ N_3(\mu \sin \gamma_3 + \cos \gamma_3) + \\ N_4(\mu \sin \gamma_4 + \cos \gamma_4) &= 6mg + Mg \dots\dots\dots(d) \\ N_1((\mu \sin \gamma_1 - \cos \gamma_1)\Gamma_x - (\mu \sin \gamma_1 + \cos \gamma_1)\Gamma_y) + \\ N_4(\Delta_{N4}^{O2} - \mu\Delta_{R4}^{O2}) &= \tau_1 + mg(\Delta_{m4}^{O2} - \Gamma_y) - Mg\Delta_M^{O2} \dots(e) \end{aligned} \right\} (1)$$

III. METHODS

A typical shrimp robot has six wheels. Its structural complexity results in a perception that it is a hard-to-build

robot. For straightforwardness, our shrimp rover is represented by a graph shown in Fig. 2. It has seven major vertices (v), including the root (v_o). Thus, the graph is a rooted type. The respective vertices or the center of rotation is summarized in Table 1. Similarly, all the other vertices are named based on the vertex number seen in Fig. 2. Except the root, all vertices represent wheels. The edges that connect between the vertices are the major structural linkages. The graph is a product of the robot constructional kinematic. It focuses on the wheels' reactions in the ground that cause a gyroscopic effect onto the bogie. This effect will in turn push to a rigorous control strategies' requirement. It is important that the bogie will maintain an upright position while roaming on an unstructured environment.

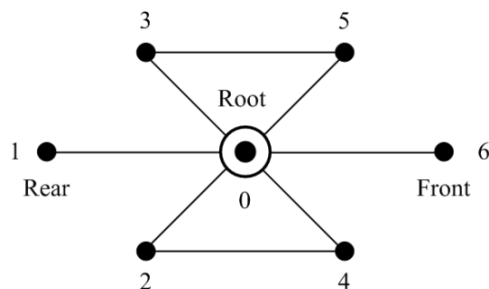


Figure 2. A simplified model of shrimp robot that is represented by a rooted graph

Definition 1: Let the wheels be designated by nodes shown in Fig. 1. Consequently, the nodes are represented by vertices of a rooted graph shown in Fig. 2.

Definition 2: Let the normal forces defined in (1) be known as the ground reaction forces. The ground reaction forces (GRFs) will be treated within the discrete events as opposed to the normal forces that are treated within the continuous events.

TABLE I. DESIGNATION OF VERTICES FOR THE SIMPLIFIED SHRIMP MECHANISM GRAPH

Vertex	Remark
0	Center of rotation
1	Rear wheel
2	Rear-pair wheel, right
3	Rear-pair wheel, left
4	Front-pair wheel, right
5	Front-pair wheel, left
6	Front wheel

Definition 3: Let the events that take place while roving is defined by a dynamic model so that all active joints respond accordingly, that the platform maintains at upright position. From (1d), we have:

$$F_{\text{front-left}} + F_{\text{front-right}} + F_{\text{rear-left}} + F_{\text{rear-right}} + (F_{\text{fork-front}} + F_{\text{absorber-front}}) + (F_{\text{fork-rear}} + F_{\text{absorber-rear}}) = M(\ddot{z}b) \quad (2)$$

$$\mathbf{F}_{v5} + \mathbf{F}_{v4} + \mathbf{F}_{v3} + \mathbf{F}_{v2} + (\mathbf{F}_{v6}) + (\mathbf{F}_{v1}) = \mathbf{m}\mathbf{a} \quad (3)$$

Proposition 1: Let the events taken place while roving, the number of possible events may be counted by a combination instantaneous reactions. For the rover, there are 64 possible combinations.

Proof: All joints of every vertex are dynamic, except the root. There exist, at least 64 possible combinations of the instantaneous reaction. There are six active vertices, where $n = 6$, because $2^n = 64$.

Definition 4: An event is designated by a membership function. A membership function (Ψ) refers to an event by a degree of instantaneous reaction force. This reference is made by real numbers -4 to 4 where $\{-4: \text{maximum low}\}$, whereas $\{4: \text{maximum high}\}$.

Proposition 2: The events that take place while roving will have induced certain degrees of reactions where (3) defines the rover behavior based on sequences within an event. We have:

$$\mathbf{H}_\Psi = \begin{bmatrix} (Q_i \times N_j), N = [f_{(v=1,\dots,6)}]; \\ f \Rightarrow F, \Psi \in \mathbb{R} | h_\Psi = \begin{cases} 4 [f] \\ 3 \uparrow \\ 2 \uparrow \\ 1 \uparrow \\ 0 \emptyset \\ -1 \downarrow \\ -2 \downarrow \\ -3 \downarrow \\ -4 [f] \end{cases} \end{bmatrix} \quad (4)$$

Proof: Suppose that the rover will roam over a rugged terrain. Therefore, all wheels will be subjected to a certain amount of GRFs such as depicted in Fig. 1, and is explained in (1). These reactions will have some degrees of forces depending on the ground contour and the rover's instantaneous speed. Using this premise, the reactions are discretized based on the degrees they reacted at that instance. So that, (3) defines that for every sequence (Q) that the rover makes, there are certain degrees of GRFs act on each wheel. A degree value (4) is a ceiling value obtained from the product of GRF and gain, whereas (-4), a floor value. These are the thresholds. The extrema are the results of the peaks and valleys of a ground contour.

IV. RESULTS AND DISCUSSIONS

The robot has a platform module with two front and rear forks. The forks have suspension modules, whereas the platform relies on the suspension given by the wheels, which is depicted in Fig. 3 exhibits. In reference to Fig. 2, the platform is represented by a root vertex. The rest of the vertices represent the wheels. Vertices 2 and 4 are dependent to one another, so do vertices 3 and 5. However, vertices 1 and 6 are independent of one another. The platform is expected to maintain a near horizontal orientation in reference to the robot frame.



Figure 3. The constructed rover.

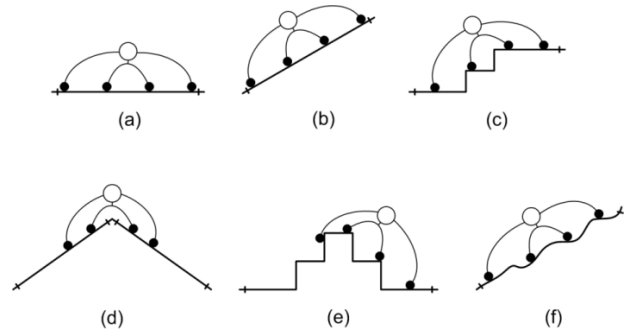


Figure 4. Maneuvering over selected ground surface profiles.

The robot with shrimp design is flexible to maneuver over rough terrains. In Fig. 4, it shows the selected profiles that robot is supposedly maneuvered. The robot would maneuver over the proposed six different ground profiles. Cases (a), (b), and (d) have flat profiles, whereas the rest of the cases have complex profiles. It is

straightforward that the condition of pair-wheel parallelism is observed in all cases. Therefore, modeling these cases using (4) resulted in (5). Equation (5) defines the wheel assembly behavior where a single row matrix describes an instantaneous sequence with respect to an individual wheel. In fact, the equation is a direct solution of (4), which is based on the unique cases exhibited in Fig. 4. The plots shown in Fig. 5 explain instantaneous sequences with respect to an individual wheel.

$$\left. \begin{aligned} H_{\psi_a} &= [0 \ 0 \ 0 \ 0 \ 0 \ 0] \\ H_{\psi_b} &= [-4 \ -3 \ -3 \ 3 \ 3 \ 4] \\ H_{\psi_c} &= [-4 \ -3 \ -3 \ 3 \ 3 \ 3] \\ H_{\psi_d} &= [-3 \ 0 \ 0 \ 0 \ 0 \ -3] \\ H_{\psi_e} &= [3 \ 4 \ 4 \ -3 \ -3 \ -4] \\ H_{\psi_f} &= [-4 \ -3 \ -3 \ 3 \ 3 \ 4] \end{aligned} \right\} \quad (5)$$

It is straightforward that for case (a), the chart illustrates the robot's orientation, positioned in a pure horizontal, where $H_{\psi_a} = [0,0,0,0,0,0]$. Similarly for case (d), the chart demonstrates the robot's orientation positioned horizontally, where $H_{\psi_d} = [-3,0,0,0,0,-3]$. The matrix elements' value at the extreme, both ends seemed to be the determinant factors that define the horizontal orientation. The condition where the robot ascends is found in cases (b), (c), and (d). The charts for these cases describe this phenomenon by "positive slope" curves. Again, it was observed that by taking the difference between the matrix elements' value at both extreme ends would determine if the robot was ascending or otherwise. Moreover, analyzing the matrix elements' value in (5) revealed some patterns that relate to the robot's behavior while roving.

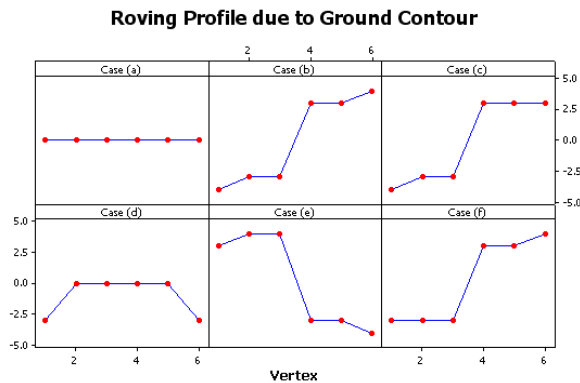


Figure 5. Simulated experiment results on which the robot maneuvered over selected ground surface profiles.

The result from the analysis is listed in Table II where every vertex is paired with each case, respectively. There is a set of rules in the last three rows. It examines whether the rear-pair wheel and the front-pair wheel are in aligned parallelisms, and whether the robot is oriented horizontally, is ascending, or is descending. The conditions are summarized by the Decision Rule 1, and are defined by (6). The data trends seen in Table II illustrate the robot behavior while in motion where Decision Rule 1 deals with the pair-wheel aligned parallelisms. Robot wobbling, on the other hand, possibly

be known by Decision Rule 2 where the instantaneous vertical component of the dynamic model defined in (1c) is made related to (5), hence (7). Likewise, robot overall behavior may be summarized by Decision Rule 3 where the conditions for pair-wheel parallelisms, climb, and tumble down are shown as a unique matrix. A similar approach was applied by Bani Hashim *et al.* [7] where they studied the biomechanical behavior human foot that was subjected to GRFs while in the stance phase.

TABLE II. DATA FOR ROBOT BEHAVIOR ANALYSIS

Vertex	Case						Remark
	a	b	c	d	e	f	
0	Center of rotation
1	0	4	-4	3	3	-4	Rear wheel
2	0	3	-3	0	4	-3	Rear-pair wheel, right
3	0	3	-3	0	4	-3	Rear-pair wheel, left
4	0	3	3	0	-3	3	Front-pair wheel, right
5	0	3	3	0	-3	3	Front-pair wheel, left
6	0	4	4	-3	-4	4	Front wheel
A	0	0	0	0	0	0	Rear-pair wheel in parallelism
B	0	0	0	0	0	0	Front-pair wheel in parallelism
C	0	∞	-7	0	7	∞	Cases (a), (d) at pure horizontal Case (e) ascends, whereas cases (b), (c), and (f) are otherwise

Decision rule 1: The platform orientation with respect to the robot frame should maintain horizontal. The orientation of the platform may be known by inspecting the elements' value for the matrix defined by (4). In addition, the difference between the matrix elements' value at both extreme ends determines if the robot was ascending or otherwise. The decision rules that determine the orientation of the robot are then defined as:

$$\left. \begin{aligned} \left| \Delta \left(h_{\psi}^{(1,2)}, h_{\psi}^{(1,3)} \right) \right| & \begin{cases} = 0 & \text{if } v_2 \text{ and } v_3 \text{ are in parallelism} \\ > 0 & \text{otherwise} \end{cases} \\ \left| \Delta \left(h_{\psi}^{(1,4)}, h_{\psi}^{(1,5)} \right) \right| & \begin{cases} = 0 & \text{if } v_4 \text{ and } v_5 \text{ are in parallelism} \\ > 0 & \text{otherwise} \end{cases} \\ \Delta \left(h_{\psi}^{(1,1)}, h_{\psi}^{(1,6)} \right) & \begin{cases} = 0 & \text{if } v_0 \text{ at pure horizontal} \\ < 0 & \text{if } v_0 \text{ ascends} \\ > 0 & \text{if } v_0 \text{ descends} \end{cases} \end{aligned} \right\} \quad (6)$$

Decision rule 2: The instantaneous dynamical response due to the normal forces possibly is known given the instantaneous behavior of the robot. Therefore, the dynamical decision rule is defined as:

$$\begin{aligned} & \left(N_1|_{-\circ h_\psi^{(1,1)}}\right)A + \left(N_2|_{-\circ h_\psi^{(1,2\wedge 3)}}\right)B + \left(N_3|_{-\circ h_\psi^{(1,4\wedge 5)}}\right)C + \\ & \left(N_4|_{-\circ h_\psi^{(1,6)}}\right)D = E \end{aligned} \quad (7)$$

We have $N_1A + N_2B + N_3C + N_4D = E$. The A, B, C, D, and E represent terms in the brackets of (1b), respectively.

Decision rule 3: Let the robot behavior while roving is defined by a decision model so that an instantaneous robot orientation may be observed. From (6) and (7), we have:

$$\mathbf{B} = \left[\begin{array}{l} \text{(Decision rule} \times \text{Case)}|_{b_{ij} \in \Delta H_\psi}|\exists \text{Case} \doteq \\ \left\{ \begin{array}{l} \text{Pair-wheel in parallelism} \\ \text{Robot ascending} \\ \text{Robot descending} \end{array} \right. \end{array} \right] \quad (8)$$

Solving for (8) and referring to Table 2, we have the solution in (9). The matrix dictates that rear and front pair wheels are in parallelism in all cases. Within the last row, the negative-valued elements represent robot ascending, whereas the positive-valued element represents robot descending. Similarly, the zero-valued elements mean the robot is positioned horizontally.

$$B = \begin{bmatrix} 0 & 0 & 0 & 0 & 0 & 0 \\ 0 & 0 & 0 & 0 & 0 & 0 \\ 0 & -8 & -7 & 0 & 7 & -8 \end{bmatrix} \quad (9)$$

V. CONCLUSIONS

Mobile robots with shrimp design are known to be ever changing when climbing or working under rough terrains. This work learnt and applied shrimp configuration to a structural and vehicular design. The orientation of the rover while in motion could be predicted by observing the patterns of membership values. It is known that gyroscopic effects on the rover are due to field surface conditions. The gyroscopic effects could be analyzed by computing the joint angles and change in heights throughout the robot maneuver. The products of joint angle and change in height represent membership

functions, which values are within certain limits. Therefore, the limits of the membership values are the determinant factors that predict the robot's stability. The decision rules may be utilized to foresee if the robot topples while roving.

ACKNOWLEDGMENT

This work was supported in part by UTeM Short-Term research grant: S00872 PJP/2011/FKP (5C).

REFERENCES

- [1] D. Songyi, L. Tao, L. Yan, L. Mengyu, and Z. Wei, "A novel shrimp rover-based mobile robot for monitoring tunnel power cables," in *Proc. International Conference on Mechatronics and Automation*, 2011, pp. 887-892.
- [2] R. Siegwart, P. Lamon, T. Estier, M. Lauria, and R. Piguat, "Innovative design for wheeled locomotion in rough terrain," *Robotics and Autonomous Systems*, vol. 40, pp. 151-162, 2002.
- [3] K. Madani and M. A. Badamchizadeh, "Mobile robot path planning based on shuffled frog leaping optimization algorithm," in *Proc. International Conference Automation Science and Engineering*, 2010, pp. 680-685.
- [4] S. Nandy, S. N. Shome, G. Chakraborty, and C. S. Kumar, "A modular approach to detailed dynamic formulation and control of wheeled mobile robot," in *Proc. International Conference Mechatronics and Automation*, 2011, pp. 1471-1478.
- [5] P. Lamon, A. Krebs, M. Lauria, R. Siegwart, and S. Shooter, "Wheel torque control for a rough terrain rover," in *Proc. IEEE International Conference in Robotics and Automation*, vol. 5, 2004, pp. 4682-4687.
- [6] K. Jong-Hwan, "Intelligence technology for cyber-physical robot system," in *Proc. International Conference on Pattern Analysis and Intelligent Robotics*, 2011, pp. 1.
- [7] A. Y. Bani Hashim, N. A. Abu Osman, W. A. B. Wan Abas, and L. A. Latif, "Approximating the relationship among the degree of the reaction forces and the nodes on footprint during a stance phase," *Applied Mathematical Modeling*, vol. 37, no. 1-2, pp. 258-264, 2013.



Ahmad Y. B. Hashim obtained his Ph.D. from the University of Malaya, M.S. degree from the Universiti Putra Malaysia, M. Edu. degree from the Universiti Teknologi Malaysia, and B.S. degree from the Pennsylvania State University. He is senior lecturer in the Department of Robotics and Automation, Faculty of Manufacturing Engineering, Universiti Teknikal Malaysia Melaka. He is now working on bioengineering, robotics, scientific computing.